

Ab initio incremental correlation treatment with non-orthogonal localized orbitals

Beate Paulus,^a Krzysztof Rościszewski,^b Hermann Stoll^c and Uwe Birkenheuer^a

^a Max-Planck-Institut für Physik komplexer Systeme, Nöthnitzer Straße 38, D-01187 Dresden, Germany

^b Institute of Physics, Jagellonian University, Reymonta 4, Pl 30-059 Krakow, Poland

^c Institut für Theoretische Chemie, Universität Stuttgart, D-70550 Stuttgart, Germany

Received 29th July 2003, Accepted 24th October 2003

First published as an Advance Article on the web 7th November 2003

The local incremental expansion of the correlation energy of extended systems is applied to non-orthogonal localized orbitals and compared to the standard approach, which uses orthogonal Foster–Boys orbitals. Several methods of how to generate suitable non-orthogonal orbitals for the investigated covalent systems, bulk silicon and beryllium rings, are discussed. For the non-orthogonal orbitals the correlation energy contributions from increments involving more than one correlated orbital decay faster with the distance between these orbitals than for standard Foster–Boys orbitals. Also, the transferability of the individual energy increments from one cluster to another cluster is better in case of the non-orthogonal orbitals. Yet, the convergence of the incremental series with the order of the increments, *i.e.* the number of correlated bonds involved, is somewhat slower compared to the orthogonal Foster–Boys orbitals.

I. Introduction

Occupied canonical molecular orbitals as obtained in *ab initio* calculations are widely used both in quantum chemistry and solid state physics (for an overview see ref. 1). They are in general delocalized over the entire system, but they can be transformed by a proper unitary transformation into a set of orthogonal localized orbitals, *e.g.* Wannier orbitals in solid state physics² or Foster–Boys orbitals in quantum chemistry.³ The orthogonality of these orbitals is not a strict requirement but (mainly due to various technical advantages) is nowadays still a rule. It is only quite recently, that Mortensen and Parrinello⁴ developed a density functional method based on localized non-orthogonal orbitals to handle large periodic systems more efficiently. A similar approach for the Hartree–Fock equations of clusters and molecules could successfully be implemented in the meantime.⁵ Localized orbitals are ideally suited for post-Hartree–Fock correlation methods because the major part of the correlation interaction in semiconductors and insulators is short-range.¹ In fact, the method of local increments⁶ just relies on this idea. It was successfully applied to a great variety of insulators^{7,8} and semiconductors,^{9,10} rare-gas crystals,¹¹ polymers¹² and graphite.¹³ The correlation energy of the *infinite* system can be obtained from a set of properly embedded finite fragments of the solid. The size of these fragments is mainly determined by the spatial extent of the localized orbitals which, at least partially, is due to the so-called orthogonalization tails of localized orbitals. The possibility of a size reduction for such fragments by the use of properly constructed non-orthogonal (and therefore overlapping) localized orbitals is the main topic of the present study. The concept of non-orthogonal (NO) localized orbitals and the idea of avoiding the orthogonalization tails of localized orbitals this way is already around for quite some time (see *e.g.* refs. 4, 14–16 and references therein). Still, NO localized orbitals have not yet found their way to standard computational schemes in quantum chemistry and solid state

physics. This may be related to the early findings of Lipscomb *et al.*¹⁵ that even optimized NO localized orbitals did not exhibit any spectacular improvement with respect to their extent as compared to the orthogonal ones. However, it has been demonstrated recently by Yang and co-workers¹⁶ that, using a different optimization scheme than in ref. 15, substantially more compact non-orthogonal localized orbitals can be generated.

To investigate the performance of the local incremental scheme with non-orthogonal orbitals, two test systems were chosen. The first one is bulk silicon, where the incremental method based on orthogonal localized Foster–Boys orbitals is known to work well.^{17,18} As the second system equidistant beryllium rings were taken where the overlap between the localized orbitals could easily be controlled by varying the Be–Be distance.

The remainder of the paper is organized as follows. In Section II the technical details of the test systems are presented. In Section III we describe the construction of the non-orthogonal localized orbitals. The results of the incremental method with the non-orthogonal orbitals are discussed in Section IV. Conclusions follow in Section V.

II. Geometries and basis sets

A. Bulk silicon

The energy increments for crystalline silicon are taken from finite Si clusters ($d(\text{Si},\text{Si}) = 2.352 \text{ \AA}$ as in bulk silicon) with the dangling bonds being saturated by tetrahedrally bound hydrogen atoms ($d(\text{Si},\text{H}) = 1.48 \text{ \AA}$ as in silane). Various different clusters have been employed, the most important ones, a compact Si_8H_{18} cluster and a zig-zag-like Si_9H_{20} cluster are shown in Figs. 1, 2 and 3 respectively. For silicon we use a scalar-relativistic pseudopotential with Ne core together with the corresponding double- ζ valence basis set¹⁹ supplemented

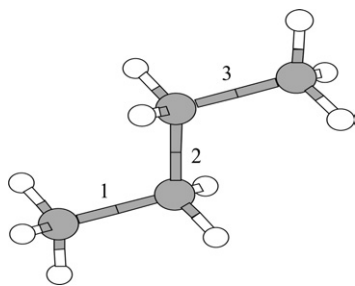


Fig. 1 Si₄H₁₀ cluster.

by one d-function (exponent 0.4). For hydrogen we took Dunning's correlation consistent [2s1p] basis set.²⁰

B. Beryllium rings

Beryllium is described by a He-core pseudopotential, because we are only interested in the properties of the valence electrons, and a (4s4p)/[2s2p] basis set.²¹ Our reference Be–Be distance was taken from the hcp (hexagonal close-packed) Be crystal ($a_0 = 2.270$ Å). The convergence of the binding energy per atom, at the CCSD (coupled-cluster with single and double excitations) level, with the length of even numbered rings is shown in Fig. 4. For rings up to Be₄₄ we also calculated the first singlet excitation energy, using the equation of motion (EOM) method at the CCSD level²² (see Fig. 4). With Be₁₈ convergence of the binding energy per atom is reached within 0.03 eV and within 0.05 eV for the first excitation energy. For this ring a series of computations with varying Be–Be distance was performed. The equilibrium distance of the Be₁₈ ring at the CCSD level is calculated to be $0.96 a_0$, *i.e.* quite close to the experimental nearest-neighbor distance in hcp beryllium.

III. Non-orthogonal localized orbitals

The guiding idea of the present study of the performance of non-orthogonal localized orbitals in the framework of the local incremental scheme is, that the NO orbitals are supposed to be more compact in space as compared to the orthogonal Foster–Boys (FB) orbitals. Various schemes to produce such non-orthogonal (NO) localized orbitals have been investigated.

The first step in the generation of NO localized orbitals is to construct, by-hand (in some way), a set of compact starting orbitals ψ_{start} such that they are quite similar to the relevant chemical bond orbitals, but still significantly more compact in space than the corresponding FB orbitals. Certainly, in general such orbitals will overlap substantially with the occupied Hartree–Fock (HF) space of the cluster, but they also will

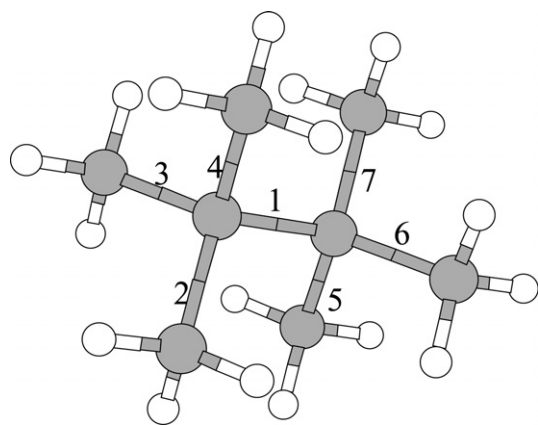


Fig. 2 Si₈H₁₈ cluster.

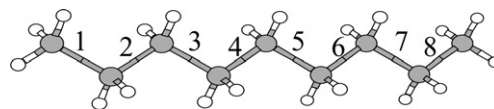


Fig. 3 Si₉H₂₀ cluster.

contain some admixture of the virtual space. To project out this virtual components from ψ_{start} we perform a Schmidt orthogonalization with respect to the virtual space

$$\psi_{\text{NO}} = \psi_{\text{start}} - \sum_{\text{virt}} \psi_{\text{virt}} \langle \psi_{\text{virt}} | \psi_{\text{start}} \rangle \quad (1)$$

for each of the individual starting orbitals ψ_{start} . Provided the hand-selected starting orbitals ψ_{start} retain their essential features during the orthogonalization (*i.e.* their nodal structure and their compactness in space), no linear dependence will occur and thus the set of projected orbitals ψ_{NO} will span the full occupied space.

The easiest way to obtain starting orbitals ψ_{start} for systems with covalent bonds, where FB localization performs well, is to simply cutoff the orthogonalization tails from the FB orbitals ψ_{FB} . Technically, this is done by setting the orbital coefficients of ψ_{FB} at those atoms not involved in the bond to zero. We will refer to this procedure as “chopping”. The resulting chopped orbitals $\psi_{\text{NO}}^{\text{chop}}$ are shown in Fig. 5 for the central bond of a Si₄H₁₀ cluster. Due to the cutting and projection, the extent of the NO orbital along the bond is reduced, while at the same time the orbital is somewhat enlarged perpendicular to the bond axis (with respect to the FB orbital). Similar findings are reported in ref. 16. The effect on the CCSD correlation energy is more pronounced. The one-bond increment to the correlation energy of the central Si–Si-bond in Si₄H₁₀ is about 15% smaller (in magnitude) than that of the FB orbital (Table 1). We attribute this loss of correlation energy to the overall reduced electron density in the chopped orbital with respect to the maximally localized Foster–Boys orbitals which causes a decrease of the correlation energy as a functional of the density. Enforcing the chopping technique by also cutting out the orbital coefficients of the outermost atomic *s* and *p* basis functions on the bond supporting silicon atoms failed. The obtained orbital $\psi_{\text{NO}}^{\text{inner}}$ was found to be almost identical to the Foster–Boys reference orbital. The overlap with the FB orbital amounts to 0.999 and the associated one-bond energy increments are practically the same for both type of orbitals (see Table. 1).

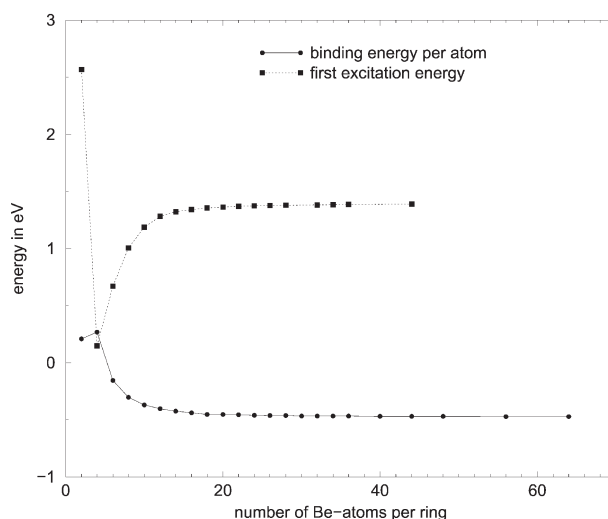


Fig. 4 Binding energy per atom and the first excitation energy of Be rings at a_0 as a function of the number of Be atoms.

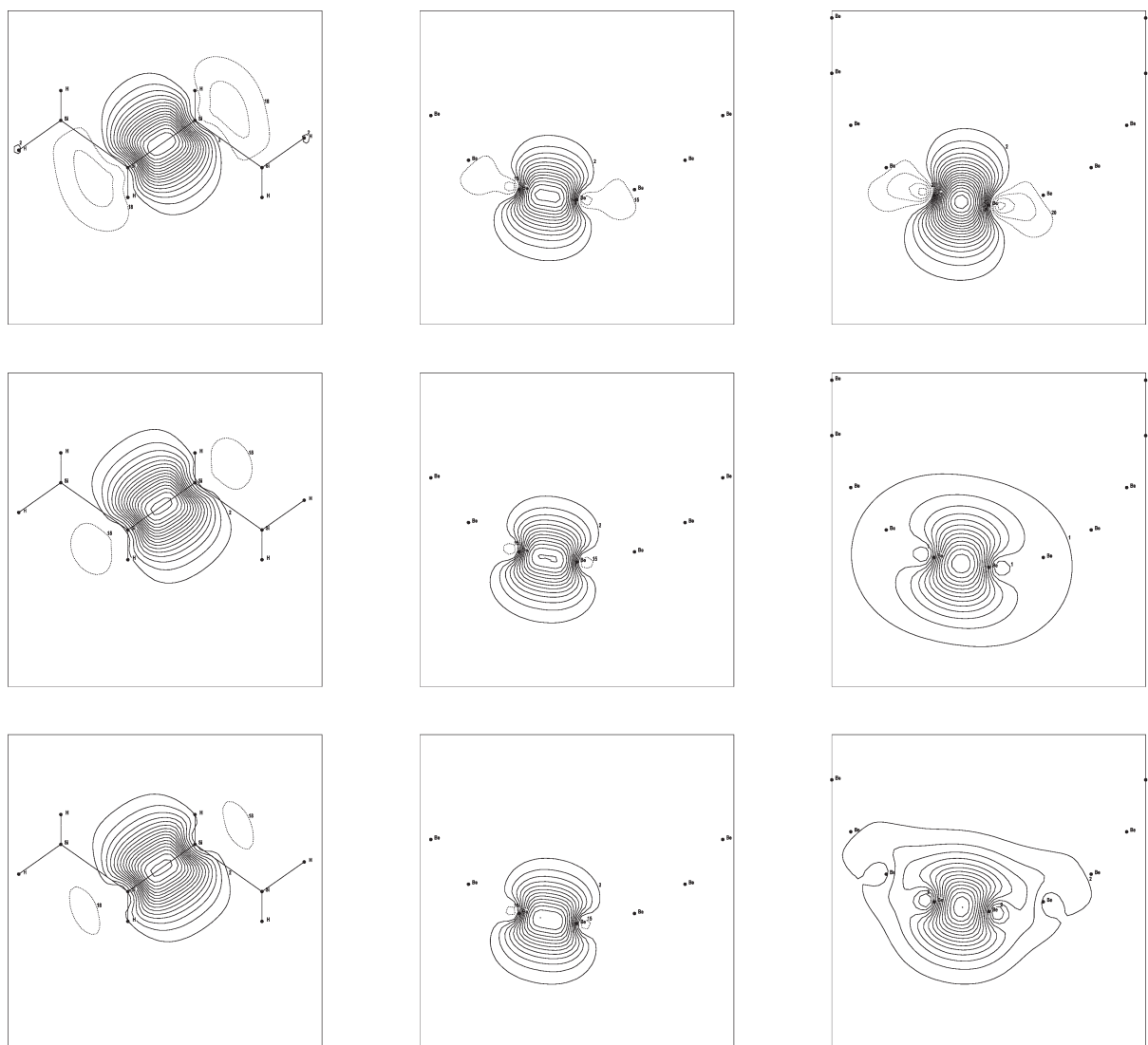


Fig. 5 Orbital plots (obtained with MOLDEN²⁴) for Si₄H₁₀ of the central Si–Si bond in Si₄H₁₀ (left) and for a Be–Be bond in Be₁₈ ring at a Be–Be distance of $a = a_0$ (middle) and $a = 0.74a_0$ (right) respectively. Shown are the FB orbitals ψ_{FB} (1st row), the normalized starting orbitals $\psi_{\text{start}}^{\text{chop}}$ with chopping technique (2nd row) and the final chopped NO orbitals $\psi_{\text{NO}}^{\text{chop}}$ (3rd row) as obtained after projection onto the occupied space. The spacing of the contours values is 0.0125 in multiples of the corresponding maximum density in all plots.

An alternative approach to non-orthogonal localized orbitals which does not require any orthogonal localized reference orbitals (such as the FB ones) is to start from classical textbook sp^3 hybrids. We extract the necessary s and p contractions from the Hartree–Fock orbitals of a single Si atom in its triplet ground state. The one-bond energy increment of the central bond of Si₄H₁₀ calculated for this hybrid-derived orbital $\psi_{\text{NO}}^{\text{hybrid}}$ is larger than that for the chopped orbital but still by 10% smaller than the value obtained for the FB orbital

Table 1 One-bond energy increments in E_{h} of the central Si–Si bond in Si₄H₁₀ together with the overlap of the NO associated orbitals with the corresponding orthogonal FB orbital and with the nearest-neighbor NO orbital (left column) for several differently constructed NO orbitals

| Orbitals | $\varepsilon(i)$ | $\langle \psi_{\text{FB}} \psi_{\text{NO}} \rangle$ | $\langle \psi_{\text{NO}}(i) \psi_{\text{NO}}(i+1) \rangle$ |
|------------------------------------|------------------|---|---|
| ψ_{FB} | −0.020841 | — | — |
| $\psi_{\text{NO}}^{\text{chop}}$ | −0.017669 | 0.974 | 0.189 |
| $\psi_{\text{NO}}^{\text{inner}}$ | −0.020821 | 0.999 | 0.012 |
| $\psi_{\text{NO}}^{\text{hybrid}}$ | −0.018641 | 0.985 | 0.126 |

(Table 1). In this sense, the hybrid-derived orbitals lay half-way between the original Foster–Boys and the chopped orbitals. Hence, for silicon we focused on the chopped orbitals $\psi_{\text{NO}}^{\text{chop}}$.

Beryllium rings do not exhibit any metallic character. Instead, the FB localization yield covalent sp -hybrid bonds for such rings which are located in between the Be atoms. We therefore applied the chopping approach also to the Be₁₈ rings. Whereas for rings at bulk Be distance $a = a_0$ qualitatively the same picture emerges as for crystalline silicon, the picture is totally different for shorter Be distances, in particular for $a = 0.74a_0$, where the first excitation energy decreases down to 0.1 eV. The starting orbital ψ_{start} obtained by cutting off the orbital coefficients is no longer more compact in space than the original Foster–Boys orbital (see Fig. 5). In addition it starts to lose its characteristic nodal structure. Upon projection the orbital enlarges even more such that the resulting chopped orbital $\psi_{\text{NO}}^{\text{chop}}$ finally extends up to the second nearest neighbors in the Be ring. Typical Be 1s core orbitals orthogonality features occur and the overlap between two neighboring chopped orbitals becomes large (0.6 for $a = 0.74a_0$). There is no reason to expect that such wide-spread orbitals perform better than the Foster–Boys orbitals in the local incremental expansion. Modifying the chopping approach by enlarging

the region of the bond supporting atoms did not improve the situation very much. The new orbitals $\psi_{\text{NO}}^{\text{chop}2}$ still exhibit second nearest neighbor overlap of more than 0.25 (see Table 2).

A more systematic approach to NO localized orbitals is to directly minimize the Foster–Boys spread functional (for normalized orbitals ψ_i)

$$\Omega[\{\psi_i\}] = \sum_i \langle \psi_i | r^2 | \psi_i \rangle - \left(\sum_i \langle \psi_i | r | \psi_i \rangle \right)^2 \quad (2)$$

without orthogonality constraints. In case of the Be rings that can be done easily because there exists only *one* symmetry-unique localized orbital. Hence, no special techniques such as those reported by Yang *et al.*¹⁶ are necessary to avoid a linear-dependence collapse during the optimization. The resulting non-linear Euler–Lagrange equation for the one normalized orbital ψ_1 reads

$$[r^2 - 2\langle \psi_1 | r | \psi_1 \rangle r] | \psi_1 \rangle = \lambda | \psi_1 \rangle \quad (3)$$

and is solved iteratively by means of successive rotations within the occupied Hartree–Fock space (similar in spirit to the self-consistent field procedure for the Hartree–Fock equation). For both Be–Be distances, the optimized NO localized orbitals $\psi_{\text{NO}}^{\text{opt}}$ are found to be surprisingly similar to the orthogonal FB orbitals (see Table 2). Apparently the shape and extent of the localized orbitals in the Be₁₈ rings is mainly determined by the occupied Hartree–Fock space of the rings rather than by the orthogonality constraints.

With the procedures described above we have a variety of NO localized orbitals at hand and can turn to the main issue of our investigation: testing the performance of non-orthogonal orbitals in the incremental expansion.

IV. The incremental expansion

A. Method

The incremental expansion for the ground state correlation energy E_{corr} of a system was described in detail in numerous papers.^{17,18} To fix the notation we only present the main equations: The correlation energy is expanded as

$$E_{\text{corr}} = \sum_i \varepsilon_i + \sum_{i<j} \Delta\varepsilon_{ij} + \sum_{i<j<k} \Delta\varepsilon_{ijk} + \dots, \quad (4)$$

where i,j,k enumerate the localized orbitals. The correlation energy increments $\varepsilon_i, \Delta\varepsilon_{ij}, \dots$ can be calculated with any size-extensive correlation method. We used the coupled cluster approach with single and double excitations (CCSD) as implemented in the program package MOLPRO.²² The one-bond increments ε_i stem from constrained correlation calculations

Table 2 One-bond energy increments in E_h in the Be₁₈ ring at two different Be–Be distances a and the overlap of the NO associated orbitals with the corresponding orthogonal FB orbital and with the first and second nearest neighboring NO orbitals for several differently constructed NO orbitals

| a | orbitals | $\varepsilon(i)$ | $\langle \psi_{\text{FB}} \psi_{\text{NO}} \rangle$ | $\langle \psi_{\text{NO}}(i) \psi_{\text{NO}}(i+1) \rangle$ | $\langle \psi_{\text{NO}}(i) \psi_{\text{NO}}(i+2) \rangle$ |
|-----------|-----------------------------------|------------------|---|---|---|
| a_0 | ψ_{FB} | −0.019867 | — | — | — |
| | $\psi_{\text{NO}}^{\text{chop}}$ | −0.019435 | 0.990 | 0.199 | 0.007 |
| | $\psi_{\text{NO}}^{\text{chop}2}$ | −0.019709 | 0.998 | 0.034 | 0.074 |
| | $\psi_{\text{NO}}^{\text{opt}}$ | −0.019672 | 0.998 | 0.109 | 0.013 |
| | $\psi_{\text{NO}}^{\text{opt}}$ | −0.024234 | — | — | — |
| $0.74a_0$ | ψ_{FB} | −0.024234 | — | — | — |
| | $\psi_{\text{NO}}^{\text{chop}}$ | −0.018910 | 0.8850 | 0.619 | 0.312 |
| | $\psi_{\text{NO}}^{\text{chop}2}$ | −0.021385 | 0.971 | 0.169 | 0.272 |
| | $\psi_{\text{NO}}^{\text{opt}}$ | −0.024198 | 0.999 | 0.018 | 0.005 |

where only the electrons from the localized orbital i are “correlated”, *i.e.* are allowed to be excited. The two-bond increments $\Delta\varepsilon_{ij}$ are defined as the non-additive contributions

$$\Delta\varepsilon_{ij} = \varepsilon_{ij} - \varepsilon_i - \varepsilon_j \quad (5)$$

to the correlation energies ε_{ij} when only orbitals i and j are correlated. In a similar way, higher order increments are defined. Note, that eqn. (5) does not account for the overlap between the localized orbitals i and j . Therefore, the incremental scheme will probably fail for strongly overlapping (and thus quite similar) orbitals i and j , because in that case $\varepsilon_{ij} \approx \varepsilon_i \approx \varepsilon_j$ is more likely to hold than the additivity assumption $\varepsilon_{ij} \approx \varepsilon_i + \varepsilon_j$.

B. Transferability

Determination of the correlation energy of an infinite solid *via* the incremental expansion requires that the energy increments extracted from different (sufficiently large) clusters essentially coincide. This transferability is necessary for extrapolating to the infinite system. Therefore it is interesting to investigate to which extent the transferability between different clusters depends on the choice of the localized orbitals. In the zig-zag Si₉H₂₀ cluster four different non-equivalent Si–Si bonds exist, and only in the compact Si₈H₁₈ cluster the central bond is fully coordinated as in bulk silicon. In Table 3 the one-bond increments and some of the two-bond increments are listed both for chopped NO orbitals $\psi_{\text{NO}}^{\text{chop}}$ and the reference Foster–Boys orbitals ψ_{FB} . The energy increments inside the clusters and between different clusters vary by at most 0.00135 and 0.00038 E_h for the one- and two-bond increments of the FB orbitals, respectively, and by 0.00070 and 0.00028 E_h for the corresponding increments of the chopped NO orbitals. Evidently, the absolute deviations of the increments are about half as large for the chopped NO orbitals than for the FB ones which is due to the orthogonalization tails of the latter orbitals. Hence, the energy increments of the chopped NO orbitals are better transferable. This feature of the NO incremental expansion would be particularly advantageous for systems where the transferability of the increments is worse than in silicon.

C. Decay with bond distance

The decay of the two-bond energy increments with increasing distance of the two bond orbitals involved has been investigated for the Si₉H₂₀ cluster and the Be₁₈ ring. The relevant data for silicon are summarized in Table 4. To reach an energy threshold of $10^{-5} E_h$ up to fourth nearest-neighbor increments have to be considered in case of the FB orbitals, whereas up to third nearest-neighbor increments are sufficient for the chopped NO orbitals. From the double logarithmic plot of this data (Fig. 6) it is clear that for the first few neighbours, at least, one has not yet reached the asymptotic limit where a

Table 3 One-bond energy increments ε_i and the nearest-neighbor two-bond increments $\Delta\varepsilon_{ij}$ both in E_h for different Si clusters obtained for the FB orbitals ψ_{FB} and the chopped NO orbitals $\psi_{\text{NO}}^{\text{chop}}$. For the bond enumeration see Figs. 1, 2 and 3

| | Cluster | Bond | ψ_{FB} | $\psi_{\text{NO}}^{\text{chop}}$ |
|--------------------------|---------------------------------|------|--------------------|----------------------------------|
| ε_i | Si ₉ H ₂₀ | 1 | −0.021123 | −0.017791 |
| | | 2 | −0.020859 | −0.017666 |
| | | 3 | −0.020863 | −0.017659 |
| | | 4 | −0.020865 | −0.017647 |
| | Si ₈ H ₁₈ | 1 | −0.019773 | −0.017088 |
| $\Delta\varepsilon_{ij}$ | Si ₉ H ₂₀ | 2 | −0.020591 | −0.017418 |
| | | 1/2 | −0.006866 | −0.006438 |
| | Si ₈ H ₁₈ | 3/4 | −0.006858 | −0.006427 |
| | | 1/2 | −0.007180 | −0.006380 |
| | | 2/3 | −0.007233 | −0.006155 |

Table 4 Two-bond energy increments $\Delta\varepsilon_{ij}$ in E_h in the zig-zag Si_9H_{20} cluster for the FB orbitals ψ_{FB} and chopped NO orbitals $\psi_{\text{NO}}^{\text{chop}}$. For the bond enumeration-see Figs. 1, 2 and 3

| | ψ_{FB} | $\psi_{\text{NO}}^{\text{chop}}$ |
|--------------------------|--------------------|----------------------------------|
| $\Delta\varepsilon_{12}$ | -0.00686527 | -0.00643669 |
| $\Delta\varepsilon_{13}$ | -0.00065549 | -0.00022024 |
| $\Delta\varepsilon_{14}$ | -0.00013539 | -0.00002719 |
| $\Delta\varepsilon_{15}$ | -0.00003118 | -0.00000744 |
| $\Delta\varepsilon_{16}$ | -0.00000850 | -0.00000223 |
| $\Delta\varepsilon_{17}$ | -0.00000248 | -0.00000071 |
| $\Delta\varepsilon_{18}$ | -0.00000079 | -0.00000025 |

van-der-Waals-like R^{-6} decay is expected:^{1,18} an average slope of -4.6 and -5.1 is found for the FB and chopped NO orbitals, respectively.

A similar behavior is seen for Be_{18} rings at $a = a_0$ (Fig. 7). Up to sixth nearest neighbors the increments of the chopped NO are smaller than the FB counterparts by about a factor of 2 while for larger distances the two types of increments approach each other again. This is because at such large distances there is no significant mutual overlap between the localized orbitals any more no matter of which kind they are. In addition, also the energy increments from the optimized NO orbitals $\psi_{\text{NO}}^{\text{opt}}$ are shown in Fig. 7. As already mentioned, they very much follow the energy increments of the orthogonal Foster-Boys orbitals. The deviation from a pure algebraic decay of the two-bond increments is quite distinct for these two types of orbitals. For the chopped NO orbitals, on the other hand, an almost algebraic decay can be observed again with an average decay exponent of -5.7 .

For Be_{18} rings with *reduced* bond length ($a = 0.74a_0$) the situation is reversed. Now the increments of the chopped NO orbitals are larger than the increments of the other types of orbitals by nearly a factor of ten. But again, no significant difference is found between the FB orbitals and the optimized NO orbitals. They both decay (on average) with an exponent of -4.9 (see Fig. 8).

The above results clearly lead to the conclusion that the intuitive expectation, that the use of non-orthogonal localized orbitals would lead to a faster decay of the two-bond increments, is only partially true. It holds for silicon where the overlap between the NO orbitals is small. Here a substantial reduction of the computational effort can be achieved, because

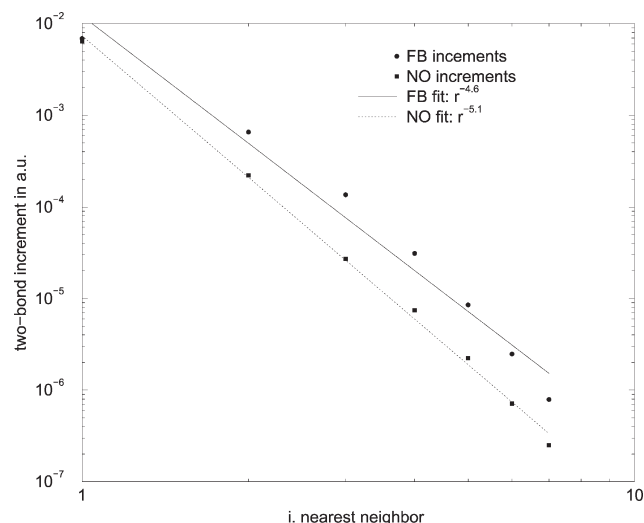


Fig. 6 Two-bond increments $\Delta\varepsilon_{1i}$ of Si_9H_{20} as function of the bond distance for the orthogonal FB orbitals ψ_{FB} and for the chopped NO orbitals $\psi_{\text{NO}}^{\text{chop}}$.

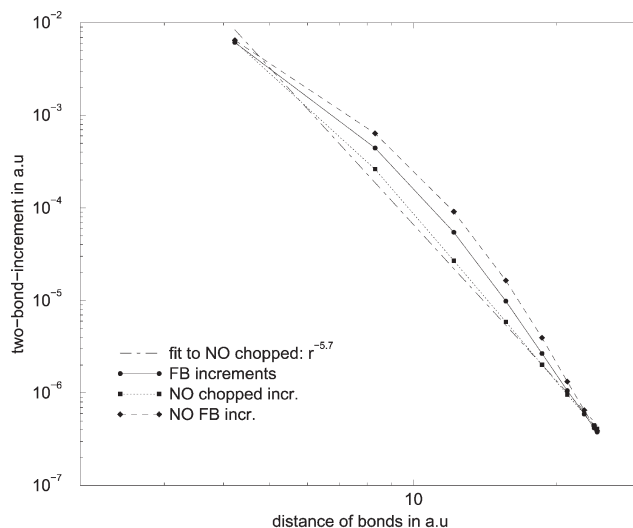


Fig. 7 Two-bond increments $\Delta\varepsilon_{1i}$ of the Be_{18} ring at $a = a_0$ as function of the spatial bond distance for orthogonal FB orbitals ψ_{FB} , the chopped NO orbitals $\psi_{\text{NO}}^{\text{chop}}$ and the optimized NO orbitals $\psi_{\text{NO}}^{\text{opt}}$.

the number of non-equivalent two-bond increments which have to be evaluated in a bulk system increases cubically with the distance of the bonds.

To a certain extent this is quite similar to the situation one encounters when switching to non-orthogonal localized orbitals in density functional calculations within the Kohn-Sham scheme as reported by Mortensen and Parrinello.⁴ The effort for the evaluation of the electron density on the numerical integration grid scales with the sixth power of the extent of the localized occupied orbitals and hence even mild improvements in the distance decay can lead to quite noticeable speed-ups.

D. Convergence with incremental order

The second important property of energy increments is their rapid decay with the number of involved orbitals, the so-called order of the increment. In Table 5 all connected, many-bond increments of the Be_{18} rings up to sixth order are listed. For higher orders the energy increments of the chopped NO orbitals are by a factor of about 10 larger than the increments of

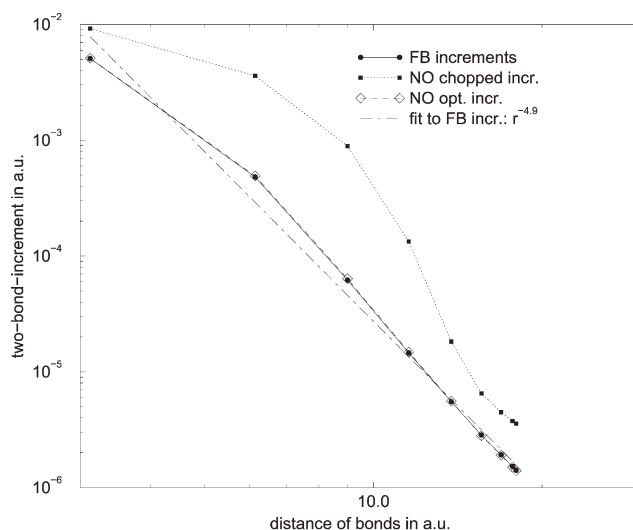


Fig. 8 Two-bond increments $\Delta\varepsilon_{1i}$ of the Be_{18} ring at $a = 0.74a_0$ as function of the spatial bond distance for the orthogonal FB orbitals ψ_{FB} , the chopped NO orbitals $\psi_{\text{NO}}^{\text{chop}}$ and the optimized NO orbitals $\psi_{\text{NO}}^{\text{opt}}$.

Table 5 Many-bond energy increments $\Delta\epsilon_{ijk\dots}$ in E_h in Be_{18} rings at two different Be–Be distances a for the FB orbitals ψ_{FB} in comparison to the chopped NO orbitals $\psi_{\text{NO}}^{\text{chop}}$ and $\psi_{\text{NO}^*}^{\text{chop}}$. For details on the $\psi_{\text{NO}^*}^{\text{chop}}$ orbitals see Section IV.D

| | $a = a_0$ | | | $a = 0.74a_0$ | |
|---------------------------|--------------------|----------------------------------|------------------------------------|--------------------|----------------------------------|
| | ψ_{FB} | $\psi_{\text{NO}}^{\text{chop}}$ | $\psi_{\text{NO}^*}^{\text{chop}}$ | ψ_{FB} | $\psi_{\text{NO}}^{\text{chop}}$ |
| $\Delta\epsilon_{123}$ | −0.0000568 | −0.0004686 | −0.0000555 | +0.0001098 | +0.0026461 |
| $\Delta\epsilon_{1234}$ | −0.0000183 | −0.0000919 | −0.0000149 | −0.0000228 | +0.0001876 |
| $\Delta\epsilon_{12345}$ | −0.0000014 | −0.0000173 | — | +0.0000003 | −0.0006519 |
| $\Delta\epsilon_{123456}$ | −0.0000009 | −0.0000037 | — | +0.0000001 | +0.0002059 |

the orthogonal Foster–Boys orbitals. As already discussed at the end of Section III this is most likely because the presence of orbital overlap is not accounted for in the definition of the higher-order increments.

Some numerical evidence for this is provided by an alternative way to evaluate the higher-order increments which avoids subtracting constrained correlation energies from overlapping orbitals. Instead of evaluating the low-order constrained correlation energies $\epsilon_i, \epsilon_{ij}, \dots$ which enter an energy increment $\Delta\epsilon_{ij}, \Delta\epsilon_{ijk}, \dots$ by using the respective subsets of *non-orthogonal* orbitals, the set of NO orbitals which defines an energy increment are Löwdin orthonormalized before and the resulting *orthogonal* orbitals are used for the constrained correlation calculations of all required orbital subsets. For example, to evaluate a two-bond energy increment $\Delta\epsilon_{ij}$ according to eqn. (5) the two NO orbitals involved, i and j are orthogonalized yielding two intermediate orthogonal orbitals i^* and j^* . The required constrained one-bond correlation energies ϵ_i and ϵ_j are then computed using these intermediate orthogonal orbitals, rather than the original ones. In fact, as can be seen from Table 5, the higher-order increments obtained this way (and referred to as chopped NO* orbitals) are as small as the corresponding Foster–Boys counterparts. However, whether an incremental series based on these modified energy increments converges to the same total correlation energy as the original series remains unclear.

In spite of the less pronounced decay of the NO energy increments with increasing order, the convergence of the incremental series is still good enough, at least for systems whose NO orbitals only exhibit small overlaps, 0.2 say, as is the case for Be_{18} rings at $a = a_0$ and for bulk silicon. This does not hold for systems with strongly overlapping localized NO orbitals such as Be_{18} rings at $a = 0.74a_0$. Although smaller than the three-bond increment the higher-order increments of the chopped NO orbitals do not show any noticeable decay with increasing order (see Table 5) and the convergence of the incremental series becomes questionable. Note, that nevertheless the *optimized* NO orbitals again essentially behave as the FB orbitals and converge quite nicely with increasing order.

The worse convergence of the incremental series with increasing order is the major drawback of the use of non-orthogonal localized orbitals for an incremental expansion, because it is computationally much more demanding to perform constrained correlation calculations for many-bond increments than to perform constrained correlation calculations for few-bond increments at larger distances.

E. The total correlation energy

The incremental scheme was developed to calculate total correlation energies of infinite systems. The results for silicon using orthogonal Foster–Boys orbitals are published in ref. 18, where the employed cluster models and the selected increments together with their symmetry weights are discussed in detail. Table 6 demonstrates how the individual energy increments (including up to 4th nearest-neighbor bonds) sum up to the total correlation per unit cell for both, the FB orbitals and the chopped NO orbitals. First note, that the total

Table 6 Total correlation energy per unit cell in E_h of Si up to the fourth order and its contributions from different incremental orders for the FB orbitals ψ_{FB} and the chopped NO orbitals $\psi_{\text{NO}}^{\text{chop}}$. The four-bond increments are restricted to connected bond configurations

| | ψ_{FB} | | $\psi_{\text{NO}}^{\text{chop}}$ | |
|------------------------------|--------------------|---------|----------------------------------|---------|
| $\sum \epsilon_i$ | −0.078932 | (42.8%) | −0.068352 | (36.9%) |
| $\sum \Delta\epsilon_{ij}$ | −0.118092 | (64.1%) | −0.097956 | (53.0%) |
| $\sum \Delta\epsilon_{ijk}$ | +0.012448 | (−6.7%) | −0.023308 | (12.6%) |
| $\sum \Delta\epsilon_{ijkl}$ | +0.000348 | (−0.2%) | +0.004672 | (−2.5%) |
| E_{corr} | −0.184228 | | −0.184944 | |

correlation energy obtained for the two kinds of orbitals coincide within less than one milliHartree, which is remarkable because *truncated* incremental series are used here to evaluate the correlation energy. However, more important in the present context is, that in the case of the chopped NO orbitals the three-bond increments count for as much as 12.6% of the total correlation energy, which is almost twice as much as in the case of the orthogonal FB orbitals. Even the few considered four-bond increments for the NO orbitals still account for 2.5% of the correlation energy (which is 0.13 eV). Hence, for highly accurate calculations they can not be neglected as is the case for the orthogonal FB orbitals.

For the Be_{18} rings the correlation energy from the incremental expansion (up to 6th order, where only the connected increment of sixth order is calculated) is compared to the correlation energy of a full standard CCSD calculation where all electrons are correlated simultaneously (see Table VII). At equilibrium distance the full correlation energy is reproduced by the incremental expansion with an error smaller than 0.02% (which is less than 2.5 meV) for both, the orthogonal FB orbitals and the chopped NO orbitals. At $a = 0.74a_0$ the FB orbitals perform even better with a energy deviation of less than 0.01% (1.0 meV), however, the error for the chopped NO orbitals is by more than one magnitude larger here (20.1 meV). The main difference between the non-orthogonal orbitals and the FB ones is the magnitude of the higher-order increments. In case of the FB orbitals the higher-order contributions account for only 0.4% of the total correlation energy for both Be distances, whereas the respective higher-order increments from the chopped NO orbitals amount for 2.4% at $a = a_0$ and for 10% even at $a = 0.74a_0$.

In summary, one can clearly state that for both systems investigated, bulk silicon and Be rings, the more the NO orbitals overlap the more important the high-order increments become.

V. Conclusions

The performance of non-orthogonal localized orbitals for an incremental expansion of the correlation energy of bulk silicon

Table 7 Total correlation energy $E_{\text{corr}}^{\text{incr}}$ in E_h for Be_{18} rings at two different Be–Be distances a and its contributions from low and high-order increments up to 6th order and 6th nearest neighbors for the FB orbitals ψ_{FB} and the chopped NO orbitals $\psi_{\text{NO}}^{\text{chop}}$. For comparison the correlation energy $E_{\text{corr}}^{\text{full}}$ for a standard CCSD calculation is given

| | $a = a_0$ | | $a = 0.74a_0$ | |
|---|--------------------|----------------------------------|--------------------|----------------------------------|
| | ψ_{FB} | $\psi_{\text{NO}}^{\text{chop}}$ | ψ_{FB} | $\psi_{\text{NO}}^{\text{chop}}$ |
| $\sum \epsilon_i + \Delta\epsilon_{ij}$ | −0.477468 | −0.468036 | −0.538092 | −0.589518 |
| $\sum \Delta\epsilon_{ijk} + \dots + \Delta\epsilon_{ijklmn}$ | −0.001890 | −0.011304 | +0.002376 | +0.053028 |
| $E_{\text{corr}}^{\text{incr}}$ | −0.479358 | −0.479340 | −0.535716 | −0.536490 |
| $E_{\text{corr}}^{\text{full}}$ | −0.479430 | | −0.535752 | |

and large Be rings have been investigated. Several recipes to generate such non-orthogonal orbitals have been tested. The most successful type of orbitals could be produced by “chopping” away the so-called orthogonality tails of precompiled orthogonal Foster–Boys orbitals. If the non-orthogonal orbitals only exhibit small mutual overlap (less than 0.2) the incremental expansion converges faster with the bond distance compared to the expansion based on orthogonal Foster–Boys orbitals. However, higher-order (more than three-bond) increments have to be taken into account in that case. For systems with significantly overlapping NO orbitals (more than 0.5) the incremental scheme with NO orbitals fails in the sense that it does not show any noticeable convergence with the order anymore.

A further advantage of non-orthogonal orbitals is their improved transferability from one model cluster to another. For bulk silicon or Be rings at equilibrium bond distance this feature is not very important, because the energy increments are well transferable in these systems even for Foster–Boys orbitals. Yet, this effect might become quite important in systems where one expects much worse transferability of the incremental contributions, such as metals which one of us has investigated recently in an alternate study.²³

Acknowledgements

The authors thank Prof. Peter Fulde (Dresden) and Dr Christa Willnauer (Dresden) for valuable suggestions and many long and helpful discussions.

References

- 1 P. Fulde, *Electron Correlations in Molecules and Solids*, Springer Series in Solid-State Sciences 100, Springer-Verlag, Berlin–Heidelberg, 3rd edn., 1995.
- 2 W. Kohn, *Phys. Rev.*, 1959, **115**, 809.
- 3 J. M. Foster and S. F. Boys, *Rev. Mod. Phys.*, 1960, **32**, 296.
- 4 J. J. Mortensen and M. Parrinello, *J. Phys. Condens. Matter*, 2001, **13**, 5731.
- 5 H. Stoll and H.-J. Werner, to be published.
- 6 H. Stoll, *Phys. Rev. B*, 1992, **46**, 6700.
- 7 K. Doll, M. Dolg, P. Fulde and H. Stoll, *Phys. Rev. B*, 1995, **52**, 4842.
- 8 K. Doll, P. Pyykkö and H. Stoll, *J. Chem. Phys.*, 1998, **109**, 2339.
- 9 B. Paulus, P. Fulde and H. Stoll, *Phys. Rev. B*, 1996, **54**, 2556.
- 10 M. Albrecht, B. Paulus and H. Stoll, *Phys. Rev. B*, 1997, **56**, 7339.
- 11 K. Rosciszewski, B. Paulus, P. Fulde and H. Stoll, *Phys. Rev. B*, 1999, **60**, 7905.
- 12 M. Yu, S. Kalvoda and M. Dolg, *Chem. Phys.*, 1997, **224**, 121.
- 13 H. Stoll, *J. Chem. Phys.*, 1992, **97**, 8449.
- 14 P. W. Anderson, *Phys. Rev. B*, 1968, **21**, 13; S. Diner, J. P. Malrieu, P. Claverie and F. Jordan, *Chem. Phys. Lett.*, 1968, **2**, 319; V. Magnasco and G. F. Musso, *J. Chem. Phys.*, 1974, **60**, 3744; P. W. Payne, *J. Am. Chem. Soc.*, 1977, **99**, 3787; E. L. Mehler, *J. Chem. Phys.*, 1977, **67**, 2728; H. Stoll, G. Wagenblast and H. Preuß, *Theor. Chem. Acc.*, 1980, **57**, 169; I. Mayer, *Chem. Phys. Lett.*, 1982, **89**, 390; G. F. Smits and C. Altona, *Theor. Chem. Acc.*, 1985, **67**, 461; F. Weinhold and J. E. Carpenter, *J. Mol. Struct.: THEOCHEM*, 1988, **165**, 189; M. Couty, C. A. Bayse and M. B. Hall, *Theor. Chem. Acc.*, 1997, **97**, 96; W. Müller, H.-J. Werner and P. Pulay, unpublished work.
- 15 K. R. Sundberg, J. Bicerano and W. N. Lipscomb, *J. Chem. Phys.*, 1979, **71**, 1515.
- 16 S. Liu, J. M. Pérez-Jordá and W. Yang, *J. Chem. Phys.*, 2000, **112**, 1634.
- 17 H. Stoll, *Chem. Phys. Lett.*, 1992, **191**, 548.
- 18 B. Paulus, P. Fulde and H. Stoll, *Phys. Rev. B*, 1995, **51**, 10 572.
- 19 A. Bergner, M. Dolg, W. Küchle, H. Stoll and H. Preuß, *Mol. Phys.*, 1993, **80**, 1431.
- 20 T. H. Dunning, *J. Chem. Phys.*, 1989, **90**, 1007.
- 21 P. Fuentealba, L. v. Szentpaly, H. Preuß and H. Stoll, *J. Phys. B*, 1985, **18**, 1287.
- 22 R. D. Amos, A. Bernhardsson, A. Berning, P. Celani, D. L. Cooper, M. J. O. Deegan, A. J. Dobbyn, F. Eckert, C. Hampel, G. Hetzer, P. J. Knowles, T. Korona, R. Lindh, A. W. Lloyd, S. J. McNicholas, F. R. Manby, W. Meyer, M. E. Mura, A. Nicklass, P. Palmieri, R. Pitzer, G. Rauhut, M. Schütz, U. Schumann, H. Stoll, A. J. Stone, R. Tarroni, T. Thorsteinsson and H.-J. Werner, *MOLPRO, a package of ab initio programs designed by H.-J. Werner and P. J. Knowles, Version 2002.1*, 2002; M. J. O. Deegan, P. J. Knowles, *Chem. Phys. Lett.*, 1994, **227**, 321.
- 23 B. Paulus, *Chem. Phys. Lett.*, 2003, **371**, 7.
- 24 G. Schaftenaar and J. H. Nordik, *J. Comput.-Aided Mol. Design*, 2000, **14**, 123.